NASA TECHNICAL MEMORANDUM

NASA TM X-2993

NASA TM X-2993

ANALOG COMPUTER IMPLEMENTATION OF FOUR INSTANTANEOUS DISTORTION INDICES

by William G. Costakis

Lewis Research Center

Cleveland, Ohio 44135

NATIONAL AERONAUTICS AND SPACE ADMINISTRATION • WASHINGTON, D. C. • MARCH 1974

1. Report No.	2. Government Accession No.	3. Recipient's Catalog No.
NASA TM X-2993		

4. Title and Subtitle	5. Report Date
ANALOG COMPUTER IMPLEMENTATION OF FOUR INSTANTANEOUS DISTORTION INDICES	March 1974
	6. Performing Organization Code

7. Author(s)	8. Performing Organization Report No.
William G. Costakis	E-7736
	10. Work Unit No. 501-24

9. Performing Organization Name and Address	11. Contract or Grant No.
Lewis Research Center National Aeronautics and Space Administration Cleveland, Ohio 44135	
	13. Type of Report and Period Covered: Technical Memorandum

12. Sponsoring Agency Name and Address	14. Sponsoring Agency Code
National Aeronautics and Space Administration Washington, D.C. 20546	

15. Supplementary Notes

16. Abstract

Dynamic distortion data obtained from inlet-engine compatibility test on a J85-GE-13 engine were used to establish the feasibility of using on-line generated indices as control signals. These data were analyzed over time increments of 1.3 seconds on an analog computer. The analog program of four instantaneous distortion indices and their results are presented. A modified approach in determining the extent of distortion is also presented.

17. Key Words (Suggested by Author(s))	18. Distribution Statement
Distortion index Dynamic distortion Instantaneous distortion	Unclassified - unlimited Cat. 28

19. Security Classif. (of this report)	20. Security Classif. (of this page)	21. No. of Pages	22. Price*
Unclassified	Unclassified	30	$3.00

* For sale by the National Technical Information Service, Springfield, Virginia 22151

ANALOG COMPUTER IMPLEMENTATION OF FOUR INSTANTANEOUS DISTORTION INDICES

by William G. Costakis
Lewis Research Center

SUMMARY

A program was conducted to test the compatibility of a J85-GE-13 engine and an axisymmetric mixed-compression inlet. The original program was designed to measure the time-variant distortion produced in a supersonic inlet and its relation to stall. Dynamic distortion data obtained from these tests were used to establish the feasibility of using on-line generated indices as control signals. An analog computer was used in the analysis for the study of long periods of time prior to stall. Dynamic distortion data obtained from these tests were analyzed over time increments of 1.3 seconds. The analog program of four instantaneous distortion indices and their results are presented. A modified approach in determining the extent of distortion is also presented.

INTRODUCTION

In recent years the distortion at the face of jet engine compressors has received a great deal of study. One of the primary goals of such studies has been to develop an empirical distortion index which could be used both to catalog the distortion generated by an inlet and also to indicate stall-producing potentials for specific engines. Such an empirical procedure, if successful, would have application in the prediction of engine-inlet compatability during inlet and engine development. This type of work normally requires a large number of dynamic sensors and is conducted in ground test facilities or on special-purpose aircraft.

In designing advanced control systems, it would be of significant value to directly sense dynamic distortion. If this were possible, the inlet and engine controls could be more closely integrated so that distortion-induced stall would be mitigated with a minimum degradation of steady-state performance. In this application, however, the number of distortion sensors must be grossly restricted to minimize the maintenance re-

quirements for a fleet of aircraft. Hence, the distortion index used for control purposes must be relatively simpler than that used to predict compatability during inlet and engine development. Although the complex indices used in compatability prediction may be applied to analyze specific distortion peaks, the simpler control index would only be expected to establish the operating regions with increased probability of encountering stall-inducing distortions.

An analog computer evaluation of several indices was performed to establish the feasibility of using on-line generated indices as control signals. Distortion data obtained from inlet-engine compatability tests run in the 10- by 10-foot Supersonic Wind Tunnel of the NASA Lewis Research Center were used. The data were originally analyzed on a digital computer, and the results of this program are presented in reference 1. The analysis of reference 1 made use of a distortion index based on screen-induced steady-state data discussed in reference 2.

In reference 1, 225 milliseconds of dynamic distortion data obtained just prior to stall were digitized. The evaluation of these data, however, was concentrated on the 40 milliseconds just prior to stall. Since the purpose of the present study was to establish the usefulness of the index as a control signal, the evaluation was extended to the 1.3 seconds prior to stall. Once the analog program was established, it was possible to investigate a number of other simple indices that could be programmed with minimal changes to the computer setup. The results obtained with four indices are thus included in this report. Although the indices evaluated may not represent desirable control signals, the results obtained could be useful in control design.

APPARATUS AND PROCEDURE

Testing and Instrumentation

The inlet used in this study was an axisymmetric mixed-compression type designed for Mach 2.5. Sixty percent of the supersonic compression was done externally. The inlet had fast-acting bypass doors for terminal shock control and a translating centerbody to effect restart and off-design operation. It, also, had provisions for both bleed and vortex generators on cowl and centerbody surfaces.

The engine used in this compatibility study was a J85-GE-13 turbojet. It has an eight-stage axial-flow compressor coupled directly to a two-stage turbine.

The compressor could be stalled by slowly closing the nozzle area while maintaining a constant engine speed. The data points investigated in this report, however, were of the drift type. That is, all facility and engine operating conditions had been set, and an equilibrium operating point had been reached, long before the compressor stalled.

Figure 1 shows the steady-state and dynamic pressure instrumentation at the com-

pressor face and compressor discharge stations. Only the fluctuating component of the dynamic data was recorded on tape. The steady-state pressures were recorded on a steady-state data recording system, and were added to the dynamic data at the time of the analysis.

The compressor face dynamic probes had a flat frequency response to 2000 hertz. The compressor discharge dynamic probes had a flat response to 300 hertz.

The dynamic portion of the data was recorded on frequency-modulated (FM) multiplexed tape at a recording speed of 152.4 cm/sec (60 in./sec). For the analog analysis presented in this report the data were tranferred from the FM multiplexed tape to a 14-channel FM tape that was compatible with the tape recorded available at the analog facility.

Description of Indices

For the implementation of the indices discussed in this report, the compressor face total-pressure instrumentation pattern was divided into five equal-area rings as shown in figure 2. A hub "super-ring" was then formed by combining rings A and B, and a tip "super-ring" was formed by combining rings D and E. Ring C was not taken into consideration in the calculation of the indices described herein. The 12 pressures in each super ring were converted into an equivalent set of six pressures by a simple radial averaging. Each of these six radially averaged pressures represents a 60° sector. The distortion was then calculated for each super ring by using the following indices:

$$\text{Index A} = \left[\frac{\overline{P_i} - P_{\min, 60^{\circ}}}{\overline{P_i}}\right] \sqrt{\frac{\beta}{180^{\circ}}}$$

$$\text{Index B} = \left[\frac{\overline{P_i} - P_{\min, 60^{\circ}}}{\overline{P_i}}\right]$$

$$\text{Index C} = \left[\frac{\overline{P_{ss}} - P_{\min, 60^{\circ}}}{\overline{P_{ss}}}\right] \sqrt{\frac{\beta}{180^{\circ}}}$$

$$\text{Index D} = \left[\frac{P_{ss} - P_{\min, 60^{\circ}}}{\overline{P_{ss}}}\right]$$

Index A is from reference 1 and indices B, C, and D are modifications of A.

These indices were applied to the hub and tip super-rings separately, and the worst indication of distortion from the two was selected.

The terms $\overline{P}_i$, $\overline{P}_{ss}$, $P_{min,\,60^o}$, and β refer to the hub or tip super-ring total pressures and the extent of distortion. The terms $\overline{P}_i$ and $\overline{P}_{ss}$ are the instantaneous and steady-state average total pressures of each super ring, respectively. And $P_{min,\,60^o}$ is the minimum 60^o sector total pressure for each super ring.

The extent of distortion β is determined from the pressure levels P_{60^o} of the 60^o sectors adjacent to the 60^o sector with the minimum pressure $P_{min,\,60^o}$ in the super-ring. Pressures adjacent to $P_{min,\,60^o}$ that are lower than the super-ring average pressure add 60^o to the extent of distortion.

This technique for determining the extent of distortion does not discriminate between small and large deviations from $\overline{P}$. There will be a number of times when the pressures adjacent to $P_{min,\,60^o}$ are slightly below $\overline{P}$ but for all practical purposes equal to $\overline{P}$. When a condition like this exists, the index considers these pressures to be below $\overline{P}$ and hence adds 60^o increments to the extent.

There were a number of ways, utilizing different curve-fitting methods that could have been used to correct this deficiency. However, these methods were judged to be too complex to be included in this study, where simplicity was of primary importance. One of the simplest methods to correct such a deficiency was to alter the extent-of-distortion determination. This was done by comparing 60^o sector pressures adjacent to $P_{min,\,60^o}$, with a percentage of $\overline{P}$. This modification reduced the probability of increasing extent by 60^o increments for small deviations from $\overline{P}$. The 60^o sector pressures adjacent to $P_{min,\,60^o}$ were compared with $\gamma\overline{P}$, where γ is the modification factor. This extent-of-distortion modification method was investigated for a range of γ from 0.90 to 1.00.

Analog Implementation of Indices

An EAI 680 analog computer was used in the implementation of the indices. Flow diagrams of the signals used in the calculation of the indices are shown in figures 3 and 4. The analog diagrams of the indices are shown in figures 5 to 8.

Figure 5 shows two of the operations in the calculation of the indices. One is the radial averaging of two pressure signals, and the other is the filtering of the radially averaged signal. Amplifiers 1 and 2 sum the steady-state and fluctuating components of the pressure signals. Amplifier 3 averages these two component signals. The averaged signal then is passed through a first-order filter. The output of the filter is a signal that represents the filtered pressure of a 60^o sector.

The portion of the filtered 60^o sector pressure that was lower than $\overline{P}$ was recorded

at all times. By recording only this portion of the signal the requirement to tell when, how long, and by how much this signal was lower than $\overline{P}$ was made easier. The zero limiter, amplifier 7, shown in figure 5 performs this function. Figure 5 represents one of six identical circuits required for a complete super-ring. The outputs of these six circuits are used in the calcualtion of $\overline{P}$, $P_{min, 60^o}$, and $\sqrt{\beta/180^o}$ shown in figures 6 to 8.

Figure 6 shows the use of logic components in the calculation of $P_{min, 60^o}$ and its rake location. Figure 7 shows the calculations of the super-ring average pressure $\overline{P}$ and the extent term $\sqrt{\beta/180^o}$. The meaning of these logic symbols and their individual functions are presented in reference 3. For a detailed discussion of the logic elements the reader is referred to reference 3 or any other compatible publication in logic circuitry. Some logic components in figures 6 and 7 are drawn in dotted lines. This means that these components were used in another circuit. For example, in figure 6 in the $P_{min, 60^o}$ rake location circuit, all comparators are dotted. This means that the signals feeding AND gates 0F, 1F, 2F, 1A, and 2A come from comparators C04, C09, C14, C19, and C24, which are part of another circuit. In this case, these comparators are part of the $P_{min, 60^o}$ circuit.

Figure 8 shows the analog diagram of the final calculation of the indices. If the instantaneous average pressure of the super-ring is fed into amplifier 50, the output of divider 53 is index B, and the output of multiplier 23 is index A. If the steady-state average pressure of the super ring is fed into amplifier 50, the output of divider 53 is index D and the output of multiplier 23 is index C.

Ideally, the hub and tip indices should be calculated simultaneously and the worst distortion between the two selected at all times and recorded. However, in the analog analysis the hub and tip indices were calculated separately because of two limitations. First, the available data for this analysis were recorded on a 14-channel analog tape recorder, with hub and tip total pressures recorded separately along with their corresponding time codes. Secondly, the analog computer used did not have sufficient logic circuitry to program the hub and tip indices simultaneously. The accuracy of the analysis did not suffer because of this. In fact, being able to observe the hub and tip indices separately may be very helpful in determining the contribution of hub and tip circumferential distortion to stall.

The hub and tip indices were recorded on a brush chart with their corresponding time codes and rake average total pressures. The hub and tip indices, then, were compared, and the worst distortion value for any desired time before stall was selected. The time code was used in selecting the exact time before stall for both indices.

RESULTS AND DISCUSSION

In this analysis the following three criteria were used in evaluating the usefulness of the indices as a control signal:

(1) The number of distortion peaks preceding stall that were higher than the stall distortion peak, where the stall distortion peak is the distortion peak established as the one causing the compressor stall in reference 1

(2) The percentage of time the index had values higher than the value of the stall distortion peak

(3) The percentage difference between the largest distortion peak encountered within a specified time and the stall distortion peak

The percentage difference is defined as $[(DP_L - DP_S)/DP_S] \times 100$, where DP_L is the value of the largest distortion peak and DP_S is the value of the stall distortion peak.

The dynamic pressure signals used in this analysis were filtered through a first-order filter with a time constant of 0.00025 second, which corresponds to 0.125 rotor revolution.

This time constant holds true for all the results presented herein unless otherwise sepecified.

Figures 9 to 12 show the instantaneous distortion for the 100 milliseconds before stall for readings 162 and 154 and indices A and C. The hub and tip super-ring indices are shown separately with their corresponding time codes, as was discussed in the section Analog Implementation of Indices. Data of this form were the basis for the evaluation of the four indices presented in this report.

In tables I to III, these three criteria are used to compare data obtained during the 125 milliseconds before stall to those obtained in the 1.3 seconds before stall for indices A and C. These tables show that the results for the 1.3 seconds before stall are not consistent with the results for the 125 milliseconds before stall.

The four indices A, B, C, and D are compared in tables IV to VI according to the criteria previously described.

The results with the modified extent of distortion for indices A and C are shown in figures 13 to 17. Figure 13 shows the results obtained for reading 162. The results obtained from index A became worse as the modification factor was varied from 1.00 to 0.97. A progressive improvement was obtained, however, as the modification varied from 0.97 to 0.90. Reading 154 is shown in figure 14. Both indices A and C improved as the modification factor was varied from 1.00 to 0.94. Reading 148 is presented in figure 15. In this case, even though index C became progressively worse with modification, it was still better than index A above 0.97 $\overline{P}$.

Reading 261 is presented in figures 16 and 17. Figure 16 shows the total index. Figure 17 shows the results of the tip index only. This reading requires special attention because of two items of special interest. For reading 261, indices A and C showed

a remarkable accuracy at zero modification (1.00 $\overline{P}$). An examination of the data showed that the P_{60^o} of rake 4 which is adjacent to $P_{min,\,60^o}$, at the time of the stall distortion peak, had a value equal to approximately 99 percent of the tip super-ring instantaneous and steady-state average total pressures. For most of the 1.3 seconds just prior to stall, the P_{60^o} of rake 4 had values equal to or higher than the tip super-ring average total pressures. And 1 percent deviation from the ring average pressure is only 0.06895 N/cm^2 (0.1 psi). Therefore, this value would hardly be considered sufficient to extend distortion an additional 60^o. Without any modification the extent of distortion at the time of the stall distortion peak is 180^o; with 1 percent modification, it is 120^o. This author believes that the extent of reading 261 is not 180^o. The extent, then, should be considered to be 120^o, because of the 60^o increments.

Index A of reading 261 is shown without modification in figure 18(a) and with 1 percent modification in figure 18(b). Figure 18(a) also shows a second large peak that was considerably reduced with the 1 percent modification. In fact, this peak required only 0.70 percent modification to bring it to the level of figure 18(b). The need for some change in the method used to determine the extent of distortion is clearly demonstrated with this reading. Reading 261 with 1 percent modification is referred to as reading 261 (modified).

The second item of interest with this reading is the excessive amount of activity in the hub index, based on reading 261 (modified). Figures 16 and 17, and the last two columns of table VI, show that distortions much higher than the stall distortion took place at the hub but stall did not occur. Since stall apparently was caused by distortion at the tip, this may indicate that distortion at the hub should be weighted differently than at the tip.

Indices B and D are formed by letting the extent factor $\sqrt{\beta/180^o}$ of indices A and C equal 1. Indices of similar form have been reported in the past (refs. 2 and 4). In this report the indices refer to hub or tip super-ring values only, while in the preceding references they refer to the whole face of the compressor. The results for indices B and D were, in general, better than the results of their corresponding indices with the extent factor, A and C, as shown in tables IV to VI. If the results of reading 261 (modified) are considered to be the correct results for this reading, based on the preceding discussion, the results of index B are consistently better than the results of index A, with the only exception occurring in reading 154 of tables IV and V. Index D showed slightly better results than index C, while the results with both C and D were better, overall, than with A and B.

In tables VII and VIII the indices are compared according to the first and third criteria, respectively, for $\tau = 0.001$ second, for the tip super-ring. The tip super-ring results are compared for this time constant, because all stalls appeared to have been caused by circumferential distortion in the tip super-ring only. A comparison of the results of indices A and B is not conclusive for this time constant. However, the results

of indices C and D were better than the results of A and B, with the only exception being reading 261. For this reading the results of index B were better than those of C for both criteria. Both indices C and D gave relatively good results. According to the first criterion, index C appears to be better than D, while according to the third criterion index D appears to be somewhat better than C.

Table IX and X show the instantaneous distortion values of the stall distortion peaks for the four indices. The results of table X differ from all previous results in that they were obtained with a time constant of 0.001 second rather than 0.00025 second. This longer time constant corresponds to approximately one-half of a rotor revolution. Table X shows that the 1 percent modification of reading 261 did not have any effect on the magnitude of the distortion peaks for $\tau = 0.001$ second. These magnitudes were already reduced considerably by the larger time constant.

The parallel compressor theory suggested in reference 5 was investigated, and the results are shown in figure 19. Steady-state hub-radial distortions affect the corrected airflow pumping capacity of the J85-GE-13 engine compressor as reported in reference 2. The compressor performance then would be different for undistorted and hub-radial distorted inflows. The compressor performance, with both undistorted and hub-radial distorted inflows, is presented in reference 1 in the form of compressor maps and stall compressor pressure ratio as a function of corrected engine speed.

Figure 19 shows these stall compressor pressure ratio lines from reference 1, with both undistorted and hub-radial distorted inflows. In addition, the four test conditions studied in the present report are shown in this figure. These four data points are the local pressure ratios of the distorted regions which are assumed to cause the stall. The compressor face total pressure used in forming these local pressure ratios was the $P_{min,\,60^o}$ at the time of the stall distortion peak of each reading. In evaluating the four data points plotted in this figure, note that a zero-angle-of-attack configuration corresponds to a condition with steady-state hub-radial distorted inflow. Thus, readings 154 and 148 must be compared to the hub-radial distorted stall line, while readings 162 and 261 must be compared to the undistorted inflow stall line.

The parallel compressor theory showed promising results in this investigation at the time of stall. However, pressure ratios, not shown in this figure, of equal magnitude or higher did occur without the compressor being affected.

If the stall lines shown in figure 19 were used as schedules in a controller designed to prevent stall, then, for every local pressure ratio above the stall line the controller would take corrective action. What is most important, however, is the fact that no stall occurred at local pressure ratios lower than the line of compressor stall pressure ratio against engine corrected speed. This means that the controller would have taken corrective action in all four cases, and the stalls might have been prevented.

CONCLUDING REMARKS

An inlet-engine compatibility test was run to determine the time-variant distortion produced in the supersonic inlet and its relation to compressor stall. Dynamic distortion data obtained in this testing were used to determine the feasibility of using four distortion indices, programmed on an analog computer, as control signals, with the following results:

1. The analog computer was found to be convenient to use and an excellent tool for the investigation of long periods of time prior to compressor stall.

2. Time periods greater than 1 second were not excessive in determining the dynamic activity of the readings.

3. The extent factor of indices A and C should be determined by a method designed to give a more accurate indication of the extent of distortion β. The modification of the average super-ring pressure in the calculation of β, used in this study, should also reduce the possibility of erroneous indications from the effect of small zero shifts in the data recording and analysis equipment on pressures equal or close to the super-ring average pressure. However, since the results of indices B and D were at least as good as, and most of the time better than, their corresponding indices with the extent factor, the extent factor could be eliminated without degradation of the results.

This conclusion applies only to these data and the way in which the results were analyzed. It is quite possible that the undesirable results obtained with the extent factor, especially for index A, may be entirely caused by the large increments of extent which were assumed.

4. Based on the data examined herein, distortion at the hub did not contribute to stall. Even in reading 261, where the hub showed considerable distortion, stall took place because of distortion at the tip. This may indicate that the distortion index should be weighted differently when applied to the hub than the tip. For this engine-inlet configuration it may be possible to completely eliminate consideration of hub distortion, which may be very important in cases where a minimum amount of instrumentation is necessary.

5. Any one of these indices may be useful in the analysis of dynamic distortion, but their close relation to engine stall was not established by these data. These indices do not appear to be useful short-time predictions of stall for use in a control system.

6. The results obtained from the application of the parallel compressor theory to these data were promising. Other pressure ratios of equal magnitude or higher were observed before stall, and thus this technique may give some false alarms. However, based on preliminary observation of the tip super-ring distortion data, the number of false alarms for the local pressure ratio was smaller than with the other indices. Considering this observation, and the fact that stalls occurred at pressure ratios equal to or higher than the expected stall pressure ratio, this technique appears promising.

If in subsequent analysis this trend holds true, the pressure ratio of the lowest compressor face pressure region may be an easy and good parameter to be used with a controller for the prevention of stall.

Lewis Research Center,
National Aeronautics and Space Administration,
Cleveland, Ohio, November 27, 1973,
501-24.

APPENDIX - SYMBOLS

DP_L	index value at largest peak
DP_S	index value at stall peak
K	potentiometer setting
N	engine speed, rpm
N^*	rated engine speed, 16 500 rpm
$\frac{N \times 100}{N^* \sqrt{\theta}}$	percentage of corrected engine speed
P	total pressure, N/m^2 (lbf/ft^2)
P_{60^o}	average pressure of a super-ring 60^o sector, N/m^2 (lbf/ft^2)
$P_{min, 60^o}$	average pressure of a super-ring 60^o sector with minimum average value, N/m^2 (lbf/ft^2)
$\overline{P}$	super-ring average total pressure, N/m^2 (lbf/ft^2)
$\overline{P}_i$	instantaneous super-ring average total pressure, N/m^2 (lbf/ft^2)
$\overline{P}_{ss}$	steady-state super-ring average total pressure, N/m^2 (lbf/ft^2)
$\overline{P}_2$	compressor face average total pressure, N/m^2 (lbf/ft^2)
$\overline{P}_3$	compressor discharge average total pressure, N/m^2 (lbf/ft^2)
s	Laplace transform variable
α	angle of attack, deg
β	extent of distortion, deg
γ	modification factor
θ	local corrected total temperature
τ	first-order filter time constant, sec

REFERENCES

1. Burstadt, Paul L.; and Calogeras, James E.: Instantaneous Distortion in a Mach 2.5, 40-Percent-Internal-Contraction Inlet and Its Effect on Turbojet Stall Margin. NASA TM X-3002, 1974.

2. Calogeras, James E.; Mehalic, Charles M.; and Burstadt, Paul L.: Experimental Investigation of the Effect of Screen-Induced Total-Pressure Distortion on Turbojet Stall Margin. NASA TM X-2239, 1971.

3. Hannauer, George: Basics in Parallel Hybrid Computer. Publ. No. 800.3039-0, Electronic Associates, Inc., Nov. 1969.

4. Reid, C.: The Response of Axial Flow Compressors to Intake Flow Distortion. Paper 69-GT-29, ASME, Mar. 1969.

5. Pearson, H.; and McKenzie, A. B.: Wakes in Axial Compressors. J. Roy. Aeron. Soc., vol. 63, no. 583, July 1959, pp. 415-416.

TABLE I. - NUMBER OF PEAKS PRECEDING STALL THAT WERE HIGHER THAN STALL DISTORTION PEAK

Reading	Index A		Index C	
	Time before stall			
	125 msec	1.3 sec	125 msec	1.3 sec
	Number of peaks preceding stall that were higher than stall distortion peak			
162	9	112	1	10
154	4	28	1	25
148	3	75	1	24
261	0	1	0	0
261 (modified)	3	69	3	72

TABLE II. - PERCENTAGE OF TIME DISTORTION WAS HIGHER THAN STALL DISTORTION PEAK

Reading	Index A		Index C	
	Time before stall			
	125 msec	1.3 sec	125 msec	1.3 sec
	Percentage of time distortion was higher than stall distortion peak			
162	2.8	4.1	0.4	0.4
154	1.2	.9	.3	.8
148	.8	3.6	.3	.8
261	.0	.0	.0	.0
261 (modified)	1.8	3.0	.8	4.5

TABLE III. - PERCENTAGE DIFFERENCE BETWEEN LARGEST PEAK AND STALL DISTORTION PEAK

Reading	Index A		Index C	
	Time before stall			
	125 msec	1.3 sec	125 msec	1.3 sec
	Percentage difference between largest peak and stall distortion peak			
162	10	23	3	11
154	14	26	3	27
148	12	85	5	55
261	0	0	0	0
261 (modified)	17	21	14	46

TABLE IV. - NUMBER OF DISTORTION PEAKS PRECEDING STALL THAT WERE HIGHER THAN STALL DISTORTION PEAK FOR 1.3 SECONDS BEFORE STALL

Index	Reading					
	162	154	148	261	261 (modified)	261 (tip only and modified)
	Number of distortion peaks preceding stall that were higher than stall distortion peak for 1.3 seconds before stall					
A	112	28	75	1	66	41
B	45	37	15	12	12	9
C	10	25	24	0	72	16
D	26	8	32	8	8	1

TABLE V. - PERCENTAGE OF TIME DISTORTION PRECEDING STALL WAS HIGHER THAN STALL DISTORTION PEAK FOR 1.3 SECONDS BEFORE STALL

Index	Reading					
	162	154	148	261	261 (modified)	261 (tip only and modified)
	Percentage of time distortion preceding stall was higher than stall distortion peak for 1.3 seconds before stall					
A	4.1	0.9	3.6	.0	3.0	1.7
B	1.5	1.0	.8	.5	.5	.4
C	.4	.8	.8	.0	4.5	.5
D	.7	.2	1.5	.3	.3	.0

TABLE VI. - PERCENTAGE OF DIFFERENCE BETWEEN LARGEST DISTORTION PEAK AND STALL DISTORTION PEAK FOR 1.3 SECONDS BEFORE STALL

Index	Reading					
	162	154	148	261	261 (modified)	261 (tip only and modified)
	Percentage of difference between largest distortion peak and stall distortion peak for 1.3 seconds before stall					
A	23	26	85	0	21	15
B	18	23	22	11	11	5
C	11	27	55	0	46	10
D	14	8	29	19	19	0

TABLE VII. - NUMBER OF DISTORTION PEAKS PRECEDING STALL THAT WERE HIGHER THAN STALL DISTORTION PEAK FOR 1 SECOND BEFORE STALL

[Time constant, 0.001 sec; tip only.]

Index	Reading			
	162	154	148	261
	Number of distortion peaks preceding stall that were higher than stall distortion peak for 1 second before stall			
A	41	55	81	51
B	46	63	22	1
C	10	25	14	14
D	19	28	21	1

TABLE VIII. - PERCENTAGE OF DIFFERENCE BETWEEN LARGEST DISTORTION PEAK AND STALL DISTORTION PEAK FOR 1 SECOND BEFORE STALL

[Time constant, 0.001 sec; tip only.]

Index	Reading			
	162	154	148	261
	Percentage of difference between largest distortion peak and stall distortion peak for 1 second before stall			
A	19	44	87	21
B	20	50	49	1
C	18	38	55	9
D	17	26	35	1

TABLE IX. - MAGNITUDE OF STALL DISTORTION PEAKS WITH TIME CONSTANT OF 0.00025 SECOND

Index	Reading				
	162	154	148	261	261 (modified)
	Magnitude of stall distortion peaks				
A	0.170	0.128	0.115	0.180	0.145
B	.172	.152	.148	.185	.185
C	.188	.145	.140	.175	.145
D	.182	.175	.150	.180	.180

TABLE X. - MAGNITUDE OF STALL DISTORTION PEAKS WITH TIME CONSTANT OF 0.001 SECOND

Index	Reading				
	162	154	148	261	261 (modified)
	Magnitude of stall distortion peaks				
A	0.155	0.072	0.075	0.145	0.145
B	.150	.085	.118	.168	.168
C	.165	.082	.095	.135	.135
D	.145	.095	.115	.156	.156

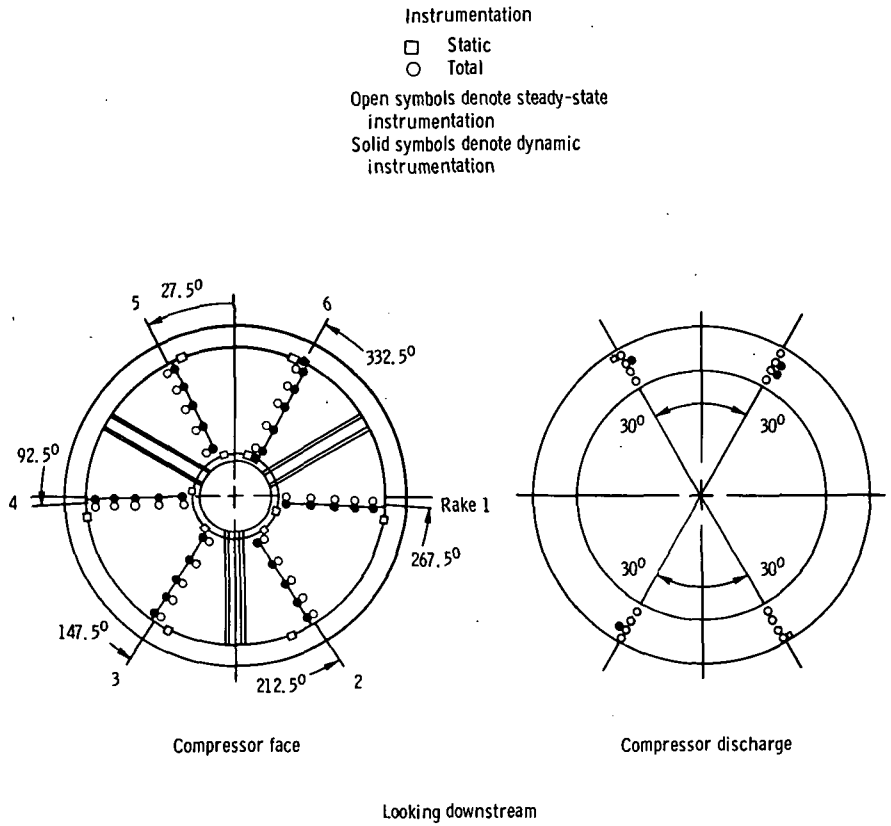

Figure 1. - Steady-state and dynamic pressure instrumentation used during test program

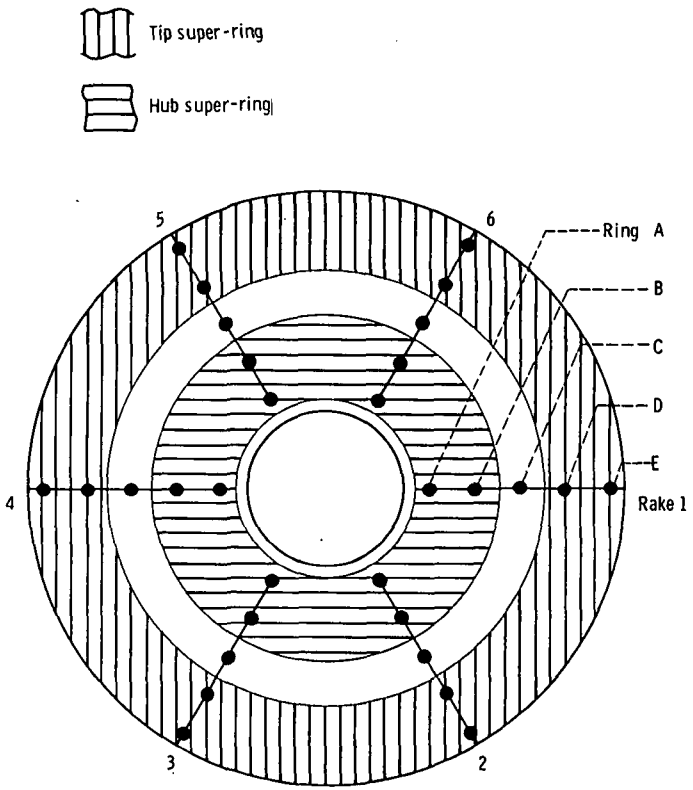

Figure 2. - Compressor face instrumentation location.

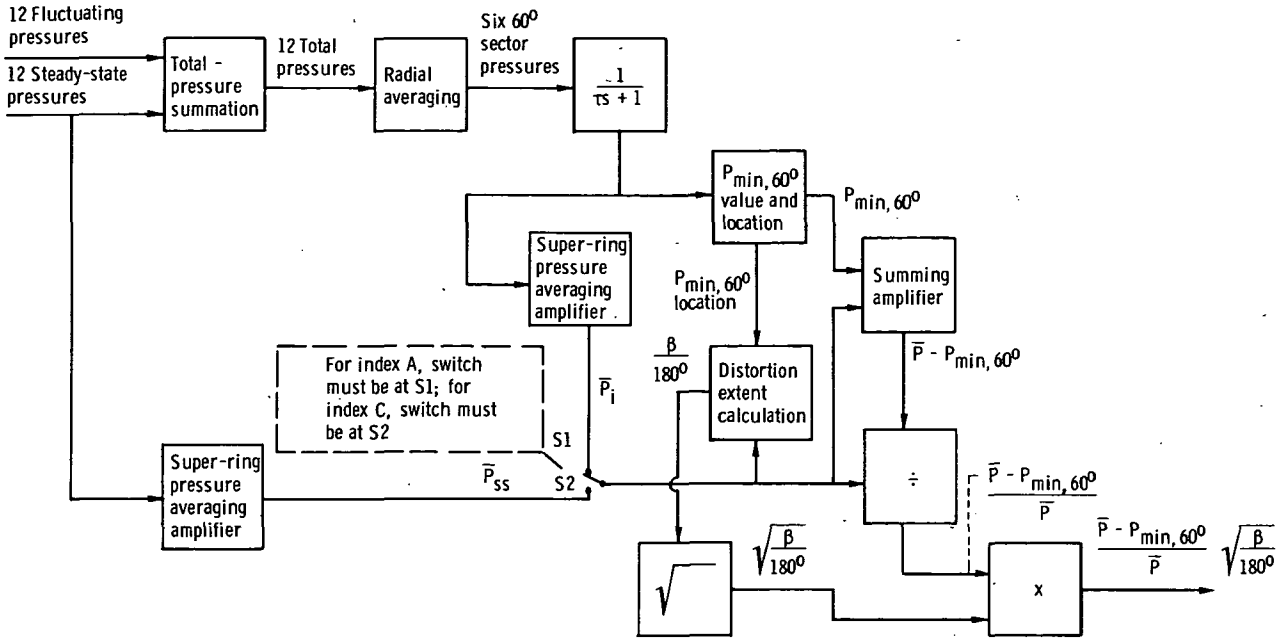

Figure 3. - Flow diagram for calculation of indices A and C.

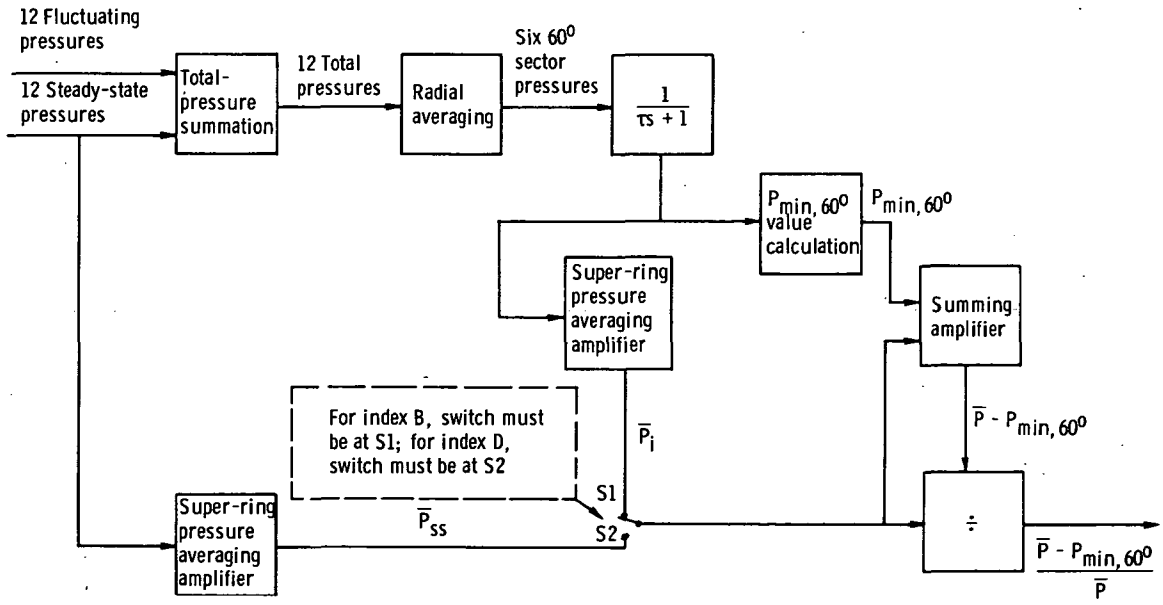

Figure 4. - Flow diagram for calculation of indices B and D.

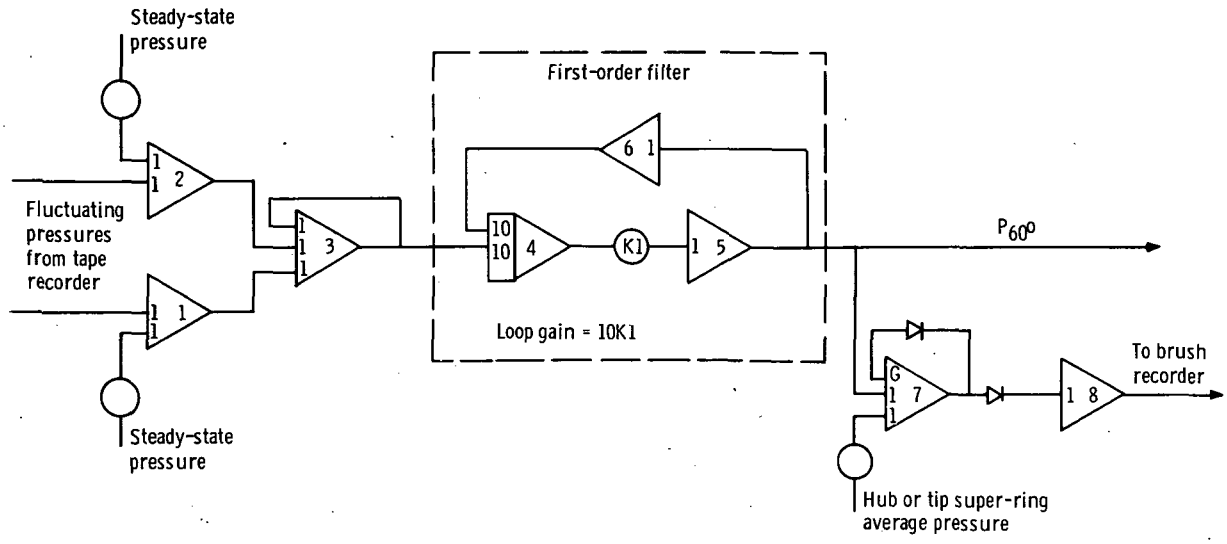

Figure 5. - Analog diagram for calculation of average pressure of a super-ring 60^0 sector P_{60^0}. (For a playback tape recorder speed of 9.525 cm/sec (3.75 in./sec), loop gain of filter is equal to 1/16 τ.)

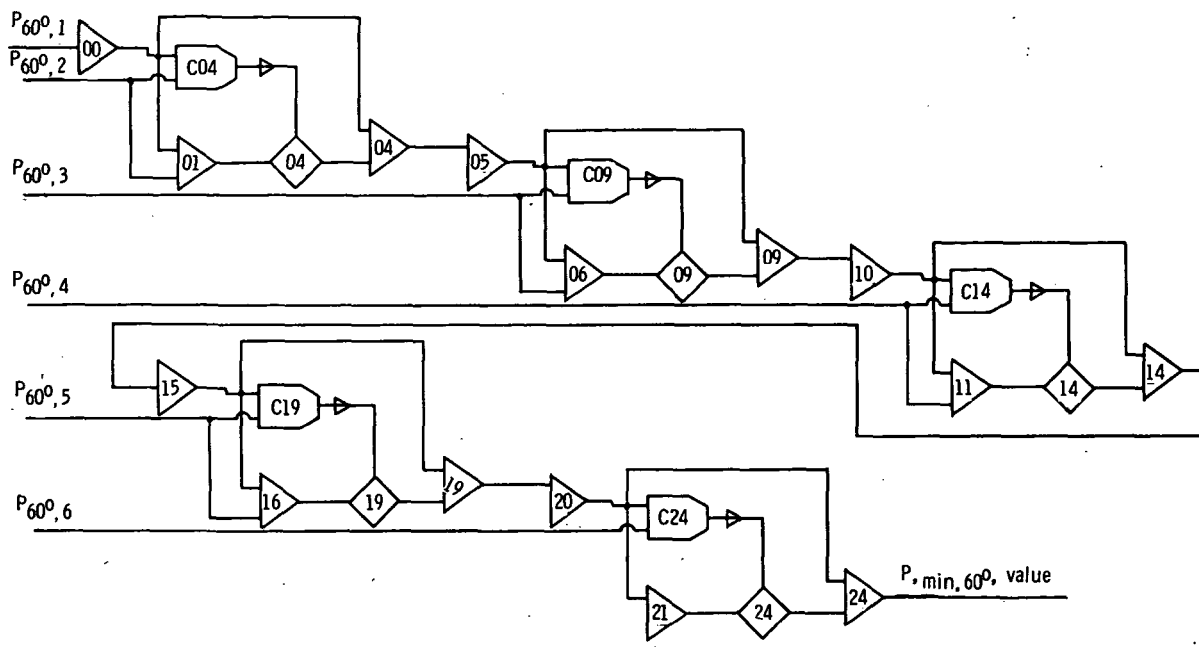

(a) $P_{min, 60^o}$ circuit.

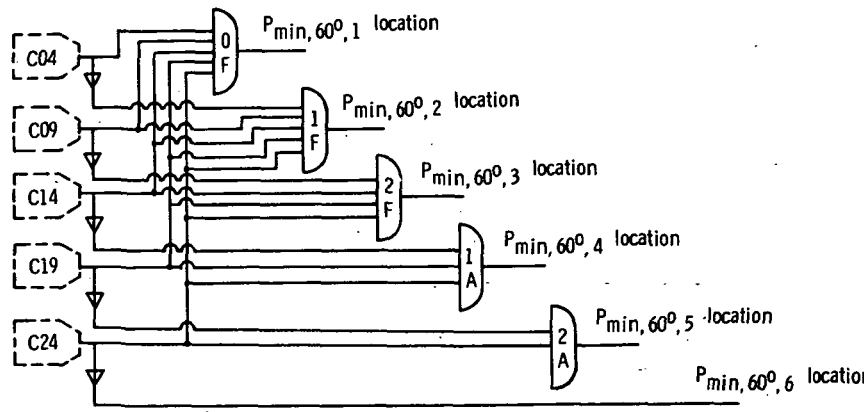

(b) $P_{min, 60^o}$ rake location circuit.

Figure 6. - Logic circuit diagram for selection of $P_{min, 60^o}$ and its location.

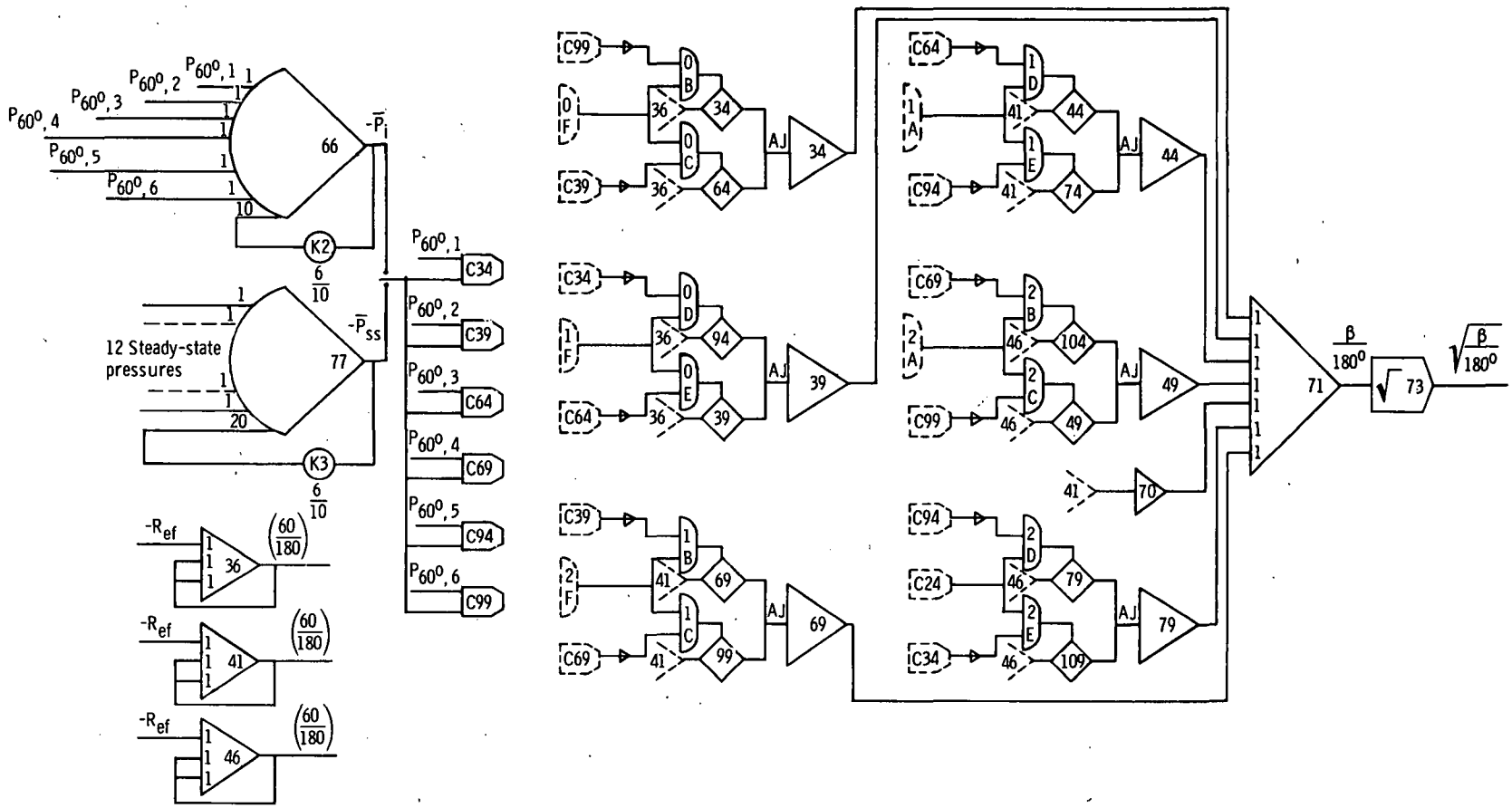

Figure 7. - Analog diagram and logic circuitry for calculation of average total pressures of the super-ring, and the extent of distortion term $\sqrt{\beta/180^0}$.

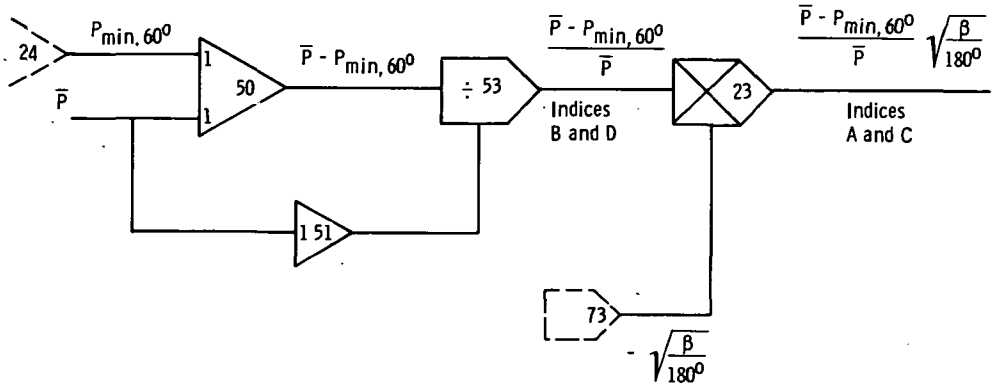

Figure 8. - Analog diagram of final calculation of indices.

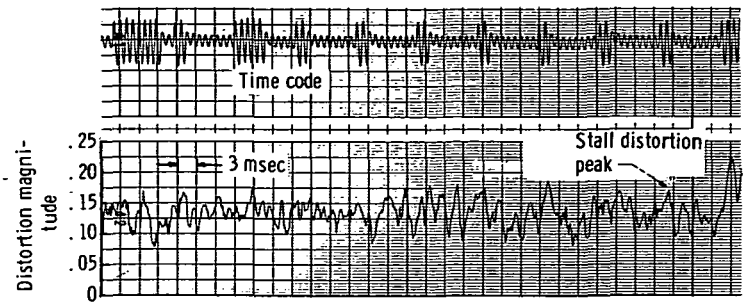

(a) Tip super-ring instantaneous distortion.

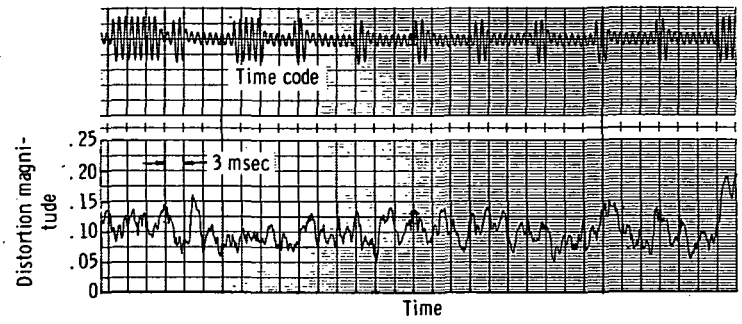

(b) Hub super-ring instantaneous distortion.

Figure 9. - Instantaneous distortion indicated by index A - reading 162. Time constant, τ, 0.00025 second.

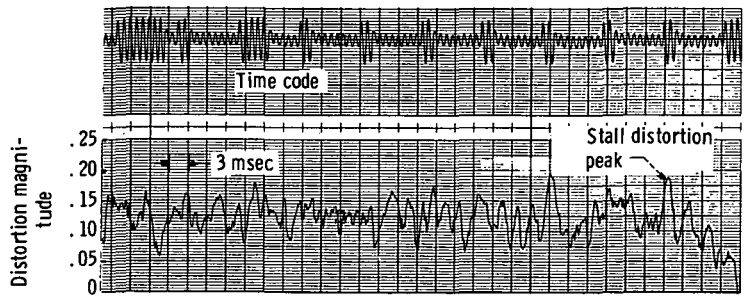

(a) Tip super-ring instantaneous distortion.

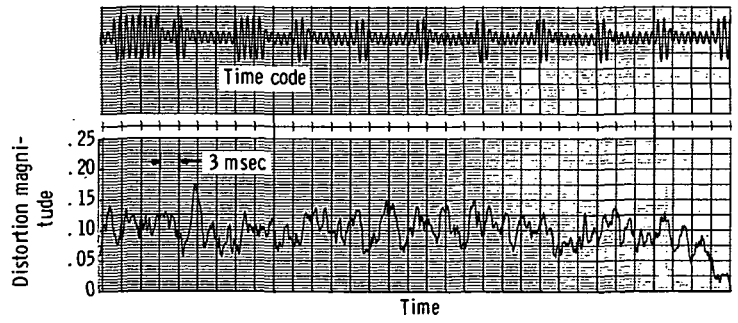

(b) Hub super-ring instantaneous distortion.

Figure 10. - Instantaneous distortion indicated by index C - reading 162. Time constant, τ, 0.00025 second.

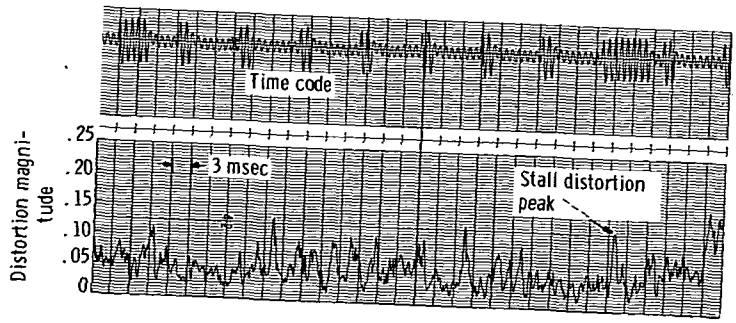

(a) Tip-super-ring instantaneous distortion.

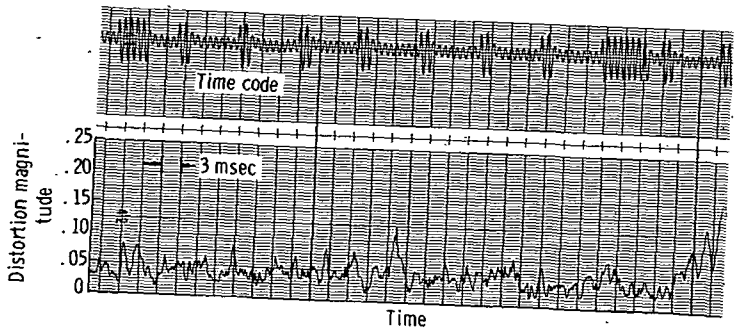

(b) Hub super-ring instantaneous distortion.

Figure 11. - Instantaneous distortion indicated by index A - reading 154. Time constant, τ, 0.00025 second.

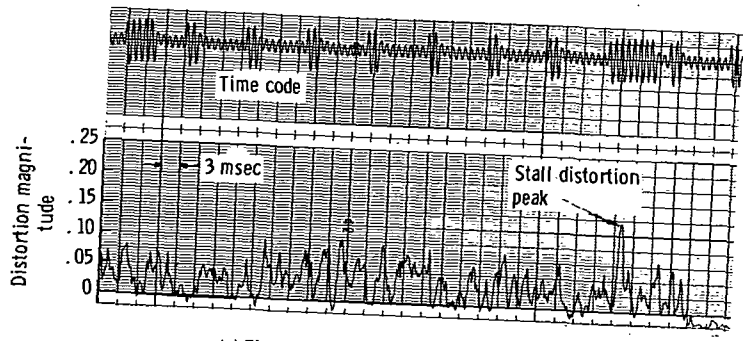

(a) Tip super-ring instantaneous distribution.

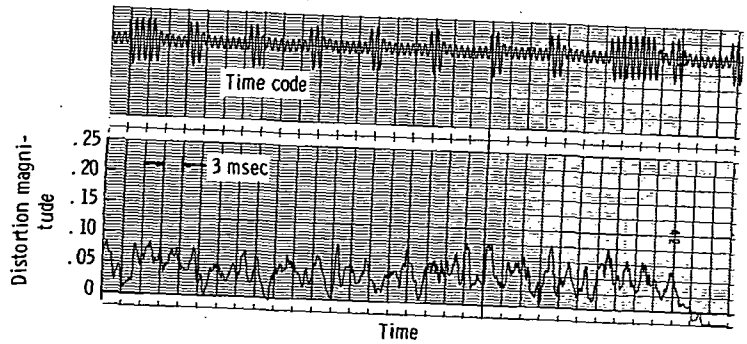

(b) Hub super-ring instantaneous distortion.

Figure 12. - Instantaneous distortion indicated by index C - reading 154. Time constant, τ, 0.00025 second.

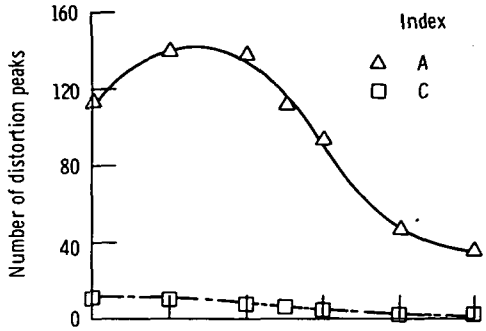

(a) Modification effect on number of distortion peaks that are larger than stall distortion peak.

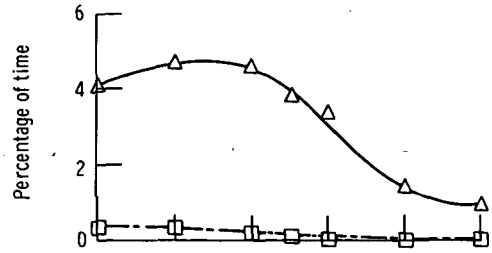

(b) Modification effect on percentage of time index had values higher than value of stall distortion peak.

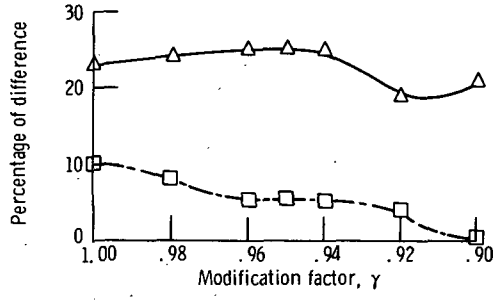

(c) Modification effect on largest distortion peak compared to stall distortion peak.

Figure 13. - Effect of modified extent of distortion β on indices A and C for reading 162.

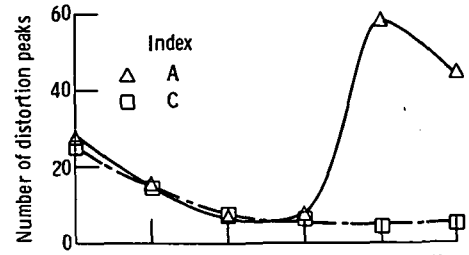

(a) Modification effect on number of distortion peaks that are larger than stall distortion peak.

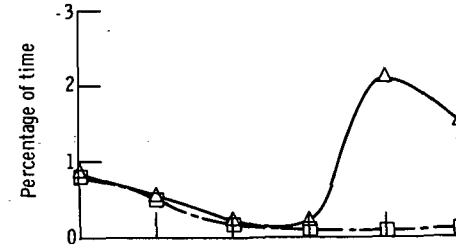

(b) Modification effect on percentage of time index had values higher than value of stall distortion peak.

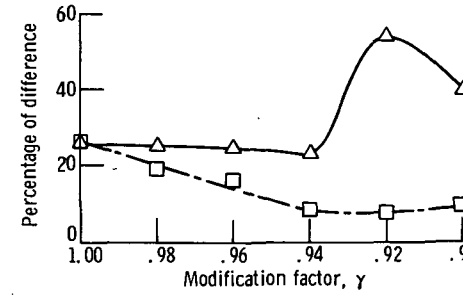

(c) Modification effect on largest distortion peak compared to stall distortion peak.

Figure 14. - Effect of modified extent of distortion β on indices A and C for reading 154.

(a) Modification effect on number of distortion peaks that are larger than stall distortion peak.

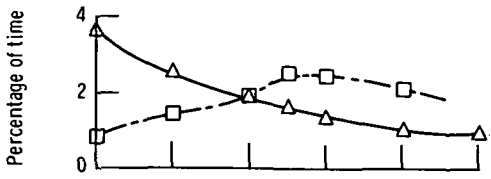

(b) Modification effect on percentage of time index had values higher than value of stall distortion peak.

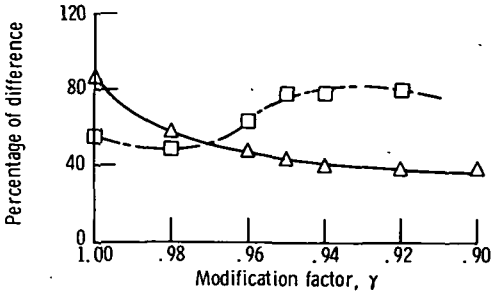

(c) Modification effect on largest distortion peak compared to stall distortion peak.

Figure 15. - Effect of modified extent of distortion β on indices A and C for reading 148.

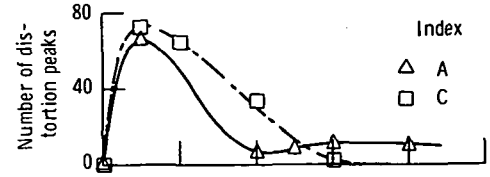

(a) Modification effect on number of distortion peaks that are larger than stall distortion peak.

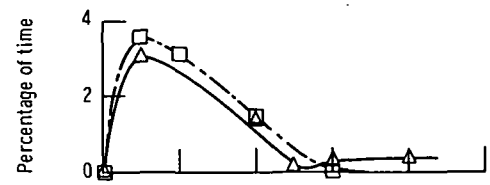

(b) Modification effect on percentage of time index had values higher than value of stall distortion peak.

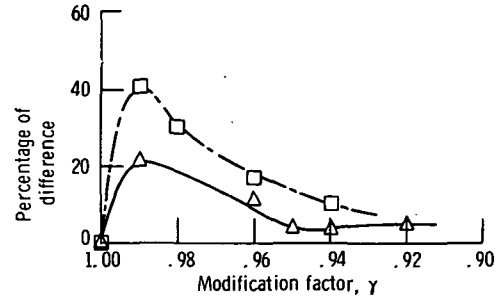

(c) Modification effect on largest distortion peak compared to stall distortion peak.

Figure 16. - Effect of modified extent of distortion β on indices A and C for reading 261.

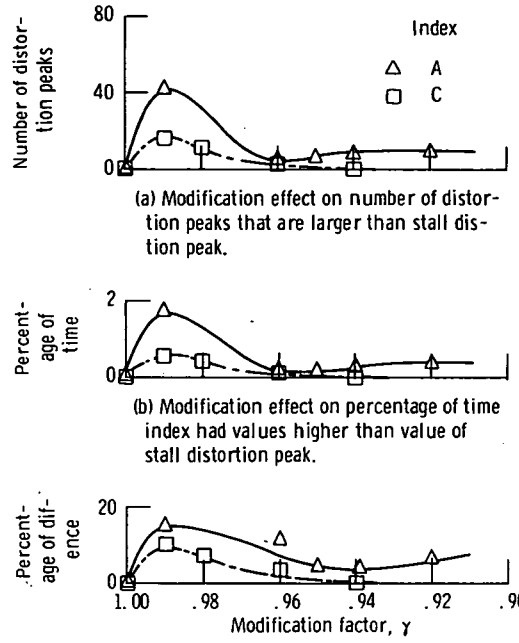

(a) Modification effect on number of distortion peaks that are larger than stall distion peak.

(b) Modification effect on percentage of time index had values higher than value of stall distortion peak.

(c) Modification effect on largest distortion peak compared to stall distortion peak.

Figure 17. - Effect of modified extent of distortion β on tip super-ring indices A and C for reading 261.

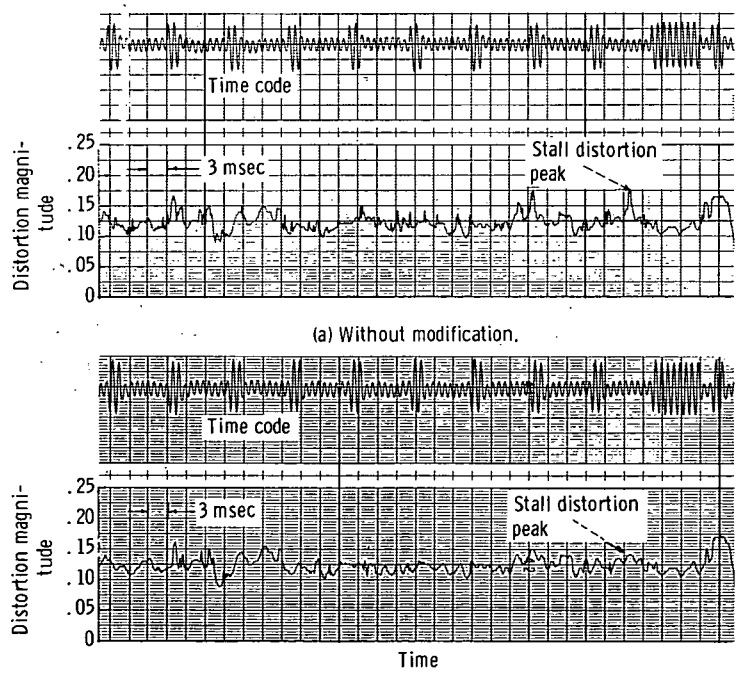

(a) Without modification.

(b) With 1 percent modification.

Figure 18. - Instantaneous distortion indicated by index A - reading 261.

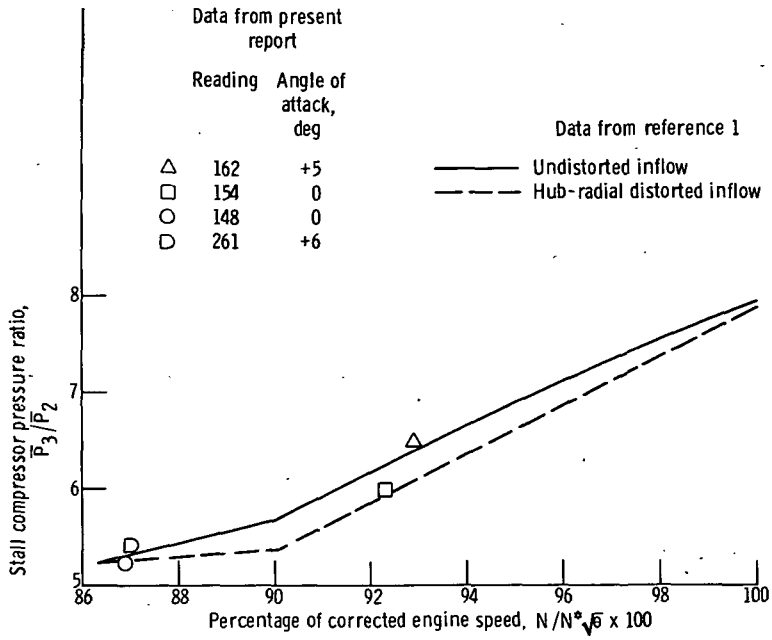

Figure 19. - Compressor pressure ratio at stall as function of corrected engine speed.

NATIONAL AERONAUTICS AND SPACE ADMINISTRATION
WASHINGTON, D.C. 20546

OFFICIAL BUSINESS
PENALTY FOR PRIVATE USE $300

SPECIAL FOURTH-CLASS RATE
BOOK

POSTAGE AND FEES PAID
NATIONAL AERONAUTICS AND
SPACE ADMINISTRATION
451

U.S.MAIL

POSTMASTER: If Undeliverable (Section 158 Postal Manual) Do Not Return

"The aeronautical and space activities of the United States shall be conducted so as to contribute . . . to the expansion of human knowledge of phenomena in the atmosphere and space. The Administration shall provide for the widest practicable and appropriate dissemination of information concerning its activities and the results thereof."

—NATIONAL AERONAUTICS AND SPACE ACT OF 1958

NASA SCIENTIFIC AND TECHNICAL PUBLICATIONS

TECHNICAL REPORTS: Scientific and technical information considered important, complete, and a lasting contribution to existing knowledge.

TECHNICAL NOTES: Information less broad in scope but nevertheless of importance as a contribution to existing knowledge.

TECHNICAL MEMORANDUMS: Information receiving limited distribution because of preliminary data, security classification, or other reasons. Also includes conference proceedings with either limited or unlimited distribution.

CONTRACTOR REPORTS: Scientific and technical information generated under a NASA contract or grant and considered an important contribution to existing knowledge.

TECHNICAL TRANSLATIONS: Information published in a foreign language considered to merit NASA distribution in English.

SPECIAL PUBLICATIONS: Information derived from or of value to NASA activities. Publications include final reports of major projects, monographs, data compilations, handbooks, sourcebooks, and special bibliographies.

TECHNOLOGY UTILIZATION PUBLICATIONS: Information on technology used by NASA that may be of particular interest in commercial and other non-aerospace applications. Publications include Tech Briefs, Technology Utilization Reports and Technology Surveys.

Details on the availability of these publications may be obtained from:

SCIENTIFIC AND TECHNICAL INFORMATION OFFICE

NATIONAL AERONAUTICS AND SPACE ADMINISTRATION

Washington, D.C. 20546